Spatial correlation of pairing modes in nuclei at finite temperature

P. Lotti and F. Cazzola
Dipartimento di Fisica, Università di Padova, Padova, Italy
and Istituto Nazionale di Fisica Nucleare, Sezione di Padova, Padova, Italy

P. F. Bortignon
Istituto di Ingegneria Nucleare, Centro Studi Nucleari Enrico Fermi, Politecnico di Milano, I-20133 Milano, Italy
and Istituto Nazionale di Fisica Nucleare, Laboratori Nazionali di Legnaro, Legnaro, Italy

R. A. Broglia
Dipartimento di Fisica, Università di Milano, Milano, Italy
Istituto Nazionale di Fisica Nucleare, Sezione di Milano, Milano, Italy
Niels Bohr Institute, Copenhagen, Denmark

A. Vitturi
Dipartimento di Fisica, Università di Trento, Povo, Trento, Italy
and Istituto Nazionale di Fisica Nucleare, Sezione di Padova, Padova, Italy
(Received 29 August 1988; revised manuscript received 14 February 1989)

We study the effect of the temperature on the spatial correlations between two nucleons, induced by the pairing interaction. Both the Cooper pairs of superfluid nuclei as well as the low-lying pairing vibrations of the normal systems are strongly affected by temperatures of the order of the pairing gap, in keeping with the close origin existing between the two modes of excitation. Giant pairing vibrations, namely the zero sound of nuclei associated with the change of particle number in two, predicted to exist in both normal and superfluid systems, are not affected by temperature.

I. INTRODUCTION

The advent of heavy-ion accelerators and of Compton-suppressed germanium detectors has allowed for the study of the nuclear structure at finite temperature and angular momentum. An important question still awaiting a simple answer is how the nucleus accommodates the angular momentum imparted to it in both grazing and fusion reactions. This question is closely related to the validity of the cranked shell model, and to the role played in nuclei by pairing correlations. In fact, the tendency towards alignment in the rotating single-particle potential is strongly quenched by the action of pairing correlations, which favor the motion of pairs of particles in time-reversal states, and the formation of a condensate. Pairing correlations in nuclei increase the probability, over that predicted by the shell model, for two nucleons moving in time-reversal orbitals to be close to each other.

These correlations are strongly affected by angular momentum and temperature. Both effects lead to a phase transition from the superfluid to the normal phase.[1] The properties of the phase transition are, however, strongly modified because of the presence of large fluctuations in particle number (cf., e.g., Refs. 2–5 and references therein). Also at rotational frequencies larger than the critical frequency ω_c, there is still an observed favoring of states where certain pairs of nucleons are coupled to angular momentum zero, over states with other couplings. Pairing vibrations[6] have been found to give rise to important renormalization of the energies and alignments for $\omega > \omega_c$ (cf., e.g., Refs. 7 and references therein).

While much effort has been dedicated to the study of the progressive blocking of pairing correlations as a function of angular momentum, less has been devoted to the behavior of pairing vibrations as a function of temperature.[8] Information on it is necessary to be able to predict and analyze the alignment of particles in hot rotating nuclei, and the limits of the cranked shell model without correlations, in nuclei rotating at frequencies and temperatures beyond the critical values at which the pairing gap collapses.

In this paper we discuss the influence of temperature in situations where the nucleus displays a static Bardeen-Cooper-Schrieffer (BCS) pairing gap, and in the case where the pairing gap being zero, well-developed pairing vibrations exist. This is done by studying the changes with temperature suffered by the spatial correlations, implied by the presence of a condensate, as well as by fluctuations of the pair field. We investigate this question in the case of both normal and superfluid systems. The two nuclei ^{208}Pb and ^{118}Sn have been chosen as paradigmatic examples of the two phases. Calculations are presented for both the condensate as well as for low-lying pairing vibrations and high-lying giant pairing resonances.[9] In Sec. II the different quantities describing the spatial correlations of the Cooper pairs are introduced and results are presented for the case of ^{208}Pb. In Sec. III the superfluid systems are discussed and numerical results presented for the case of ^{118}Sn. The conclusions are presented in Sec. IV.

II. PAIR DENSITY: NORMAL SYSTEMS

A selective way to reveal the collectivity of the pairing modes is to study the spatial correlation of nucleons moving in time-reversal state, a property which is specifically probed in the transfer of two nucleons.

In the case of an uncorrelated s pair of nucleons and fixing the position of one of them at a given point in the nucleus, the probabilities to find the second close to the first or on the opposite side of the nucleus, are equal. Pairing correlations lead to a marked increase of the probability for the two particles to move close to one another.[10–12]

For two nucleons coupled to total angular momentum $I=0$ and spin $S=0$, the spatial distribution may be defined as

$$P(\mathbf{r}_1,\mathbf{r}_2)=|\delta\rho_{S=0}(\mathbf{r}_1,\mathbf{r}_2)|^2 , \tag{1}$$

where

$$\delta\rho_{S=0}(\mathbf{r}_1,\mathbf{r}_2)=\langle[a^\dagger(\mathbf{r}_1,\sigma_1)a^\dagger(\mathbf{r}_2,\sigma_2)]_{I,S=0}\rangle_T = \frac{1}{4\pi}\sum_j A_j^{(pv)}R_{n_jl_j}(r_1)R_{n_jl_j}(r_2)P_{l_j}(\cos\theta_{12}) \tag{2}$$

is the thermal average of the two-particle transfer operator. The operator $a^\dagger(\mathbf{r},\sigma)$ creates a particle at the point $\mathbf{r}$ in space with spin σ, $a^\dagger(\mathbf{r},\bar{\sigma})$ being the corresponding time-reversal operator and $[a^\dagger a^\dagger]_{I,S=0}$ the singlet component of the monopole ($I=0$) Cooper pair creation operator. The index j labels the single-particle levels, while the quantities $R_{n_jl_j}(r)$ are the single-particle radial wave functions. The detailed expression of the quantities $A_j^{(pv)}$ are given case by case in what follows.

As an example of a normal system displaying strong pairing correlations, we consider ^{210}Pb, i.e., two neutrons moving around a closed shell. The amplitudes $A_j^{(pv)}$ were obtained in the particle-particle thermal random phase approximation (pp-RPA) making use of the standard pairing Hamiltonian, and are given by[8,13]

$$A_j^{(pv)}=\frac{\Lambda_+^{(pv)}Q_j}{2\epsilon_j-W_+^{(pv)}}\left[\frac{\Omega_j}{4\pi}\right]^{1/2}(1-2n_j) . \tag{3}$$

The quantities Q_j are the matrix elements of the radial form factor, $\Omega_j=j_j+\frac{1}{2}$, and $\Lambda_+^{(pv)}$ is a normalization constant for the solution with energy $W_+^{(pv)}$. In the expression for the $A_j^{(pv)}$ the quantities $\Lambda_+^{(pv)}$, $W_+^{(pv)}$, and n_j depend on the temperature T; in particular, n_j is the familiar thermal occupation factor for the single-particle level with energy ϵ_j,

$$n_j=\frac{1}{1+\exp\left[\frac{\epsilon_j-E_F}{T}\right]} . \tag{4}$$

To evidence the effect of the pairing interaction, the probability distribution associated with the correlated pp-RPA solution at $T=0$ (Fig. 1, middle), is compared with the corresponding quantity associated with the two neutrons moving in the pure $1g_{9/2}$ orbit (Fig. 1, left). In this case the probability distribution for the second particle resembles the associated single-particle density, which is independent of the position of the first particle. In the correlated case the probability distribution of the second particle is concentrated around the first particle. The presence of components in the mixed wave function corresponding to orbitals with both parities breaks the sym-

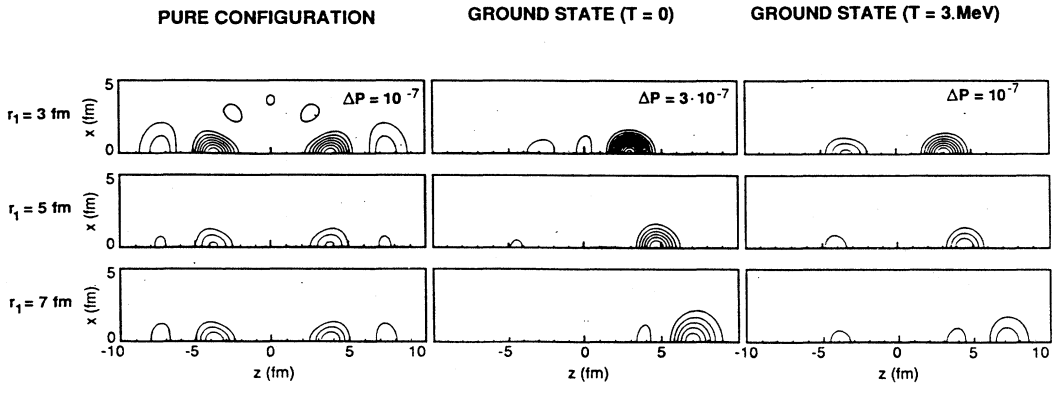

FIG. 1. Contour plot of the two-particle probability distribution for the ground state of ^{210}Pb. The function $P(\mathbf{r}_1,\mathbf{r}_2)$ is displayed in the x-z plane for different fixed values of $\mathbf{r}_1$ as a function of the position $\mathbf{r}_2$ of the other particle (because of the symmetry of the problem, only half of the plane is shown). The position of the first particle on the z axis is indicated at the left-hand side of the figure. The $A_j^{(pv)}$ coefficients have been obtained within the pp-RPA formalism, with the inclusion of the temperature (Refs. 8 and 13). The single-particle levels have been generated in the Hartree-Fock approximation with a SK III interaction and constraining the nucleus in a box of large radius. The strength of the pairing interaction has been fixed as to reproduce the experimental binding energy of the ground state of ^{210}Pb. The left-hand side refers to the uncorrelated case, corresponding to two particles moving in the $1g_{9/2}$ orbital. The differential increment ΔP of each contour curve is marked at the right top of the figures. In the case of zero temperature, these contours coincide with those displayed in Ref. 12.

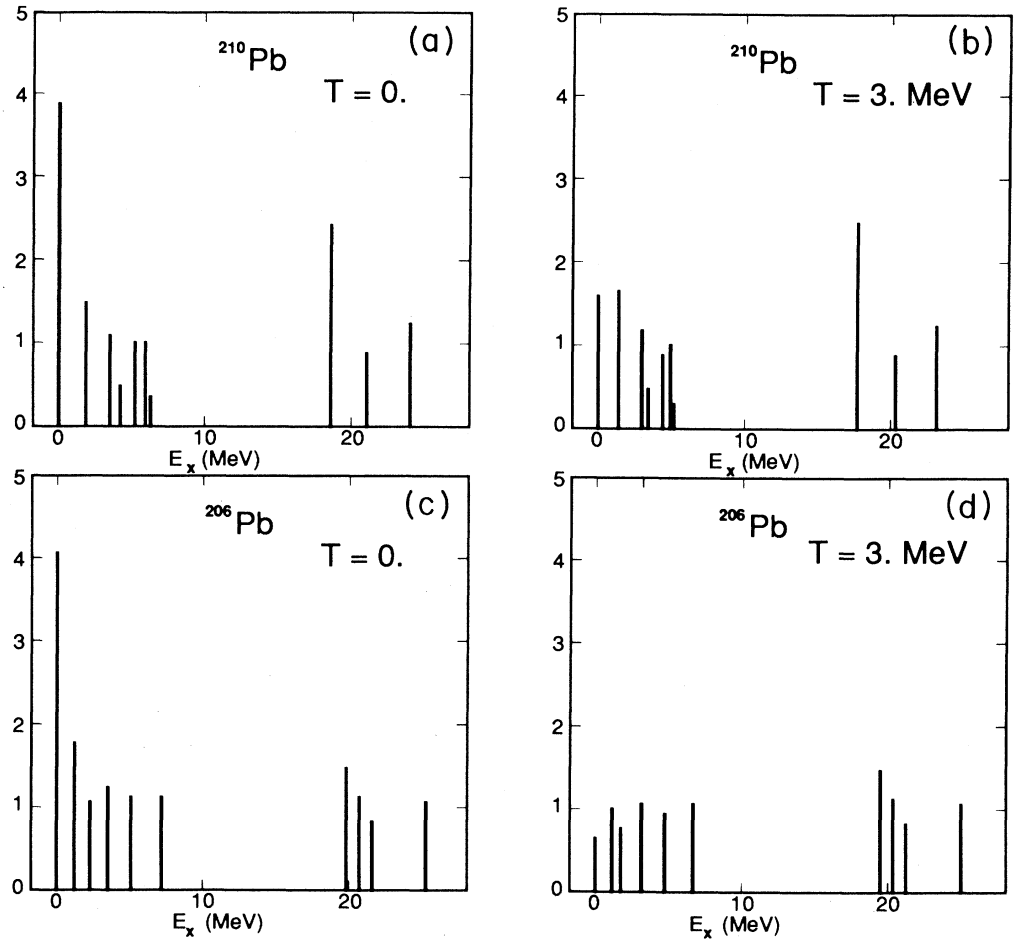

FIG. 2. Distribution of pairing strength obtained in pp-RPA for the addition [(a) and (b)] and removal modes [(c) and (d)] as a function of the energy of the modes. In both cases both the $T=0$ and $T=3$ MeV results are shown.

metry with respect to the center of the nucleus, strongly inhibiting configurations where the two particles are on the opposite sides of the nucleus.[10–12]

A similar situation applies also for the giant pairing vibrations expected in the high-lying part of the nuclear spectrum. These excitations are a simple consequence of the shell structure, and are expected to renormalize, in an important way, the two-nucleon transfer cross section associated with the low-lying modes (cf. Ref. 9). Attempts to detect them have been carried out (cf. Ref. 14). However, the bombarding conditions were rather marginal in these experiments, also because giant pairing vibrations

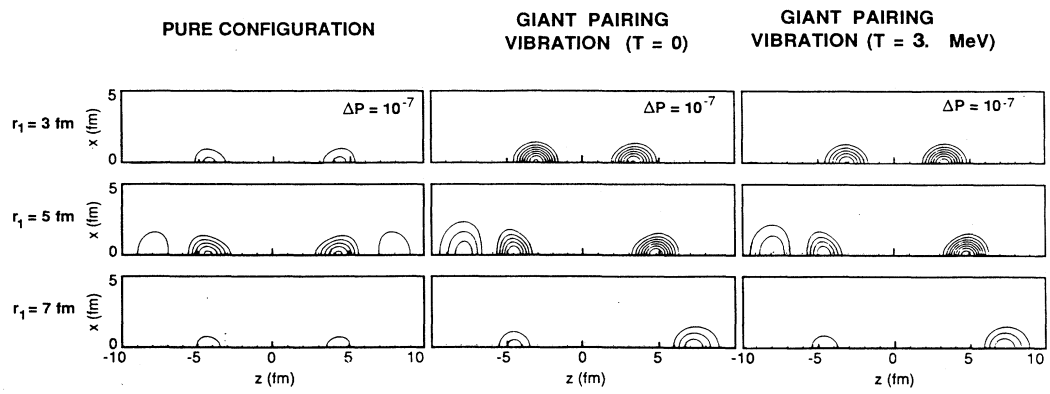

FIG. 3. Two-particle contour plots associated with the giant pairing vibrational state in ^{210}Pb. In this case the corresponding pure configuration (displayed on the left side) is the $(1h_{11/2})^2$. For details see the caption to Fig. 1.

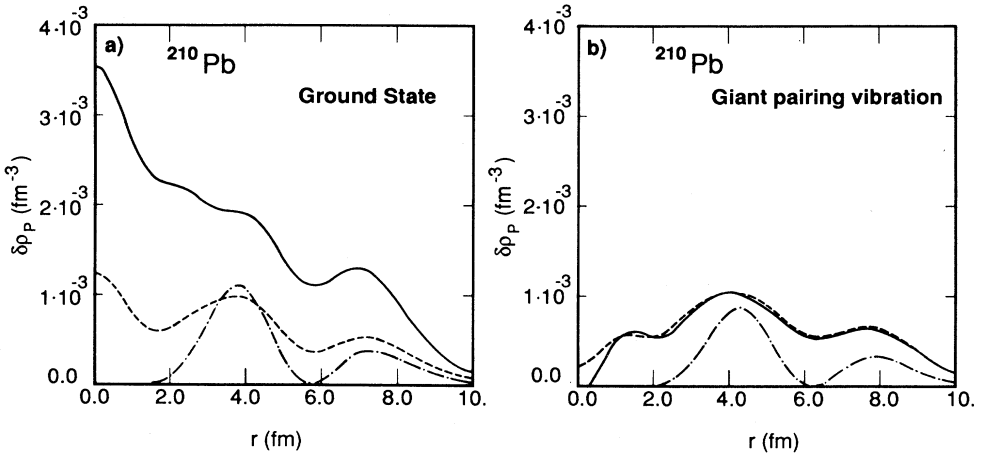

FIG. 4. Local transition densities associated with the addition modes in ^{210}Pb. The densities are displayed in (a) and (b) for the ground state and the giant pairing mode, respectively. In both cases the predictions of the pp-RPA calculation at zero and finite temperature ($T=3$ MeV), solid and dashed lines, respectively, are compared with the analogous quantities associated with the uncorrelated wave functions, dashed-dotted line. For details on the pp-RPA calculation see the caption to Fig. 1.

are expected to display a sizable damping width (cf. Ref. 9).

As apparent from the distributions of pairing strength obtained in the pp-RPA and displayed in Fig. 2(a), the shell structure gives rise to high-lying states in ^{210}Pb characterized by strengths comparable with those of the corresponding ground states.[9,15] The strength distribution gives also indication of the degree of collectivity of the high-lying pairing modes. It is obtained from the matrix element of the two-particle creation operator between the ground state and the excited states,

$$T_{+}^{(pv)} = \langle \sum_j [a_j^\dagger a_j^\dagger]_{I,S=0} \rangle_T = \sum_j \frac{\Lambda_{+}^{(pv)} Q_j}{2\epsilon_j - W_{+}^{(pv)}} \left[\frac{\Omega_j}{4\pi} \right]^{1/2} (1-2n_j) , \quad (5)$$

which in the case of pickup reactions becomes equal to

$$T_{-}^{(pv)} = \langle \sum_j [a_j a_j]_{I,S=0} \rangle_T = \sum_j \frac{\Lambda_{-}^{(pv)} Q_j}{2\epsilon_j - W_{-}^{(pv)}} \left[\frac{\Omega_j}{4\pi} \right]^{1/2} (1-2n_j) . \quad (6)$$

The two-particle correlation plot is shown in Fig. 3 (middle) for the most collective high-lying state which we can associate with the giant pairing vibration. As in the case of the low-lying pair vibration, the effect of the collectivity is clearly evidenced by the comparison with the analogous quantity associated with the uncorrelated wave function, displayed on the left side of Fig. 3. Note that, owing to the details of the shell structure, no indication for high-lying collective states is found in the strength distribution for the removal modes, displayed in Fig. 2(c).

In Fig. 2 we also show the strength distributions obtained for addition and removal modes for $T=3$ MeV. In both cases no appreciable variations are detectable in the higher part of the spectrum, leaving practically unaffected both position and strength of the giant pairing vibration associated with the addition mode. As a consequence the associated two-particle correlation plots, displayed on the right side of Fig. 3, are very similar to those obtained at $T=0$. Variations with the temperature are present in the lower part of the spectrum, which is more sensitive to changes in the occupation factors around the Fermi surface. The overall temperature dependence observed here is rather similar to that found in the case of particle-holes modes.[16] There is in fact a redistribution of the strength among the different states, with the result of a reduction of the collectivity. The associated weakening of the pair cluster is evident by comparing the two last columns of Fig. 1.

In Fig. 4 we show the square of the local pair transition density[17]

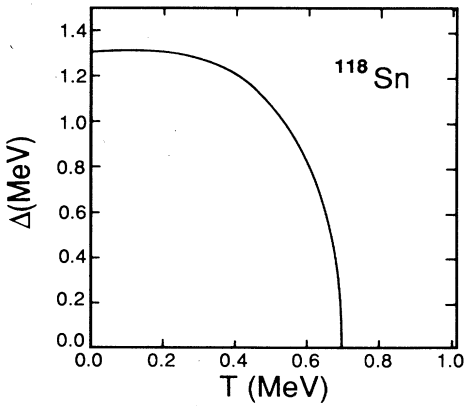

FIG. 5. The pairing gap Δ as a function of the temperature for ^{118}Sn. The single-particle levels have been generated in the Hartree-Fock approximation with a SK III interaction and constraining the nucleus in a box of large radius. For the pairing strength the value $G_0=0.139$ MeV has been used.

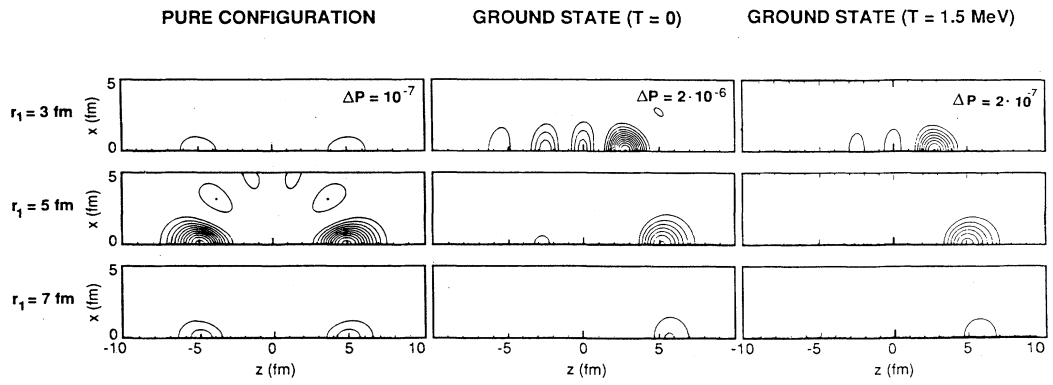

FIG. 6. Two-particle correlation plots associated with the BCS ground state, for different values of the position of the first particle, at zero and finite temperatures (middle and right-hand side). The left-hand side refers to the case of uncorrelated particles, which in this case are expected to move in the $0h_{11/2}$ orbital.

$$\delta\rho_{S=0}(\mathbf{r}) \equiv \delta\rho_{S=0}(\mathbf{r},\mathbf{r}) = \langle [a^{\dagger}(\mathbf{r},\sigma)a^{\dagger}(\mathbf{r},\sigma)]_{I,S=0} \rangle_T = \frac{1}{4\pi} \sum_j A_j^{(pv)} R_j^2(r) , \quad (7)$$

where the above-mentioned effects of the temperature are clearly displayed.

III. SUPERFLUID SYSTEMS

We consider now open-shell nuclei described within the BCS approximation. As an example we have taken the nucleus ^{118}Sn, which at zero temperature displays features characteristic of the superfluid phase. The pairing gap,

$$\Delta = G \sum_j \Omega_j u_j v_j (1-2f_j) , \quad (8)$$

is shown as a function of temperature in Fig. 5. In Eq. (8) the quantity

$$f_j = \frac{1}{1+\exp\left[\frac{E_j}{T}\right]} \quad (9)$$

is the thermal quasiparticle occupation factor, E_k being the quasiparticle energy. As shown in the figure, the function $\Delta(T)$ displays a transition from superfluid to normal phase at a temperature $T \approx 0.7$ MeV. This result is consistent with those obtained in previous works.[18,19] This estimate of critical temperature, at $A \approx 120$, for the collapse of the nuclear pairing gap leads to the relation

$$\Delta(0) \approx 1.80 k_B T_c .$$

The characteristic value of $\Delta(0) \approx 1.26$ MeV has been derived considering that the Debye energy of the lowest normal modes of a rotationally invariant nuclear core is found to be $\omega_D \approx 4.4$ MeV (Ref. 18) and that the following relationship holds:

$$\frac{1}{N(0)|V(0)|} = \int_0^{\omega_D/2k_B T_c} \frac{dx}{x} \tanh x = \ln\left[\frac{2e\gamma_E}{\pi}\frac{\omega_D}{k_B T_c}\right] ,$$

where $N(0)$ is the density of states per unit volume, $V(0)$ is the momentum space pairing potential for low momentum values, and γ_E the Euler constant.

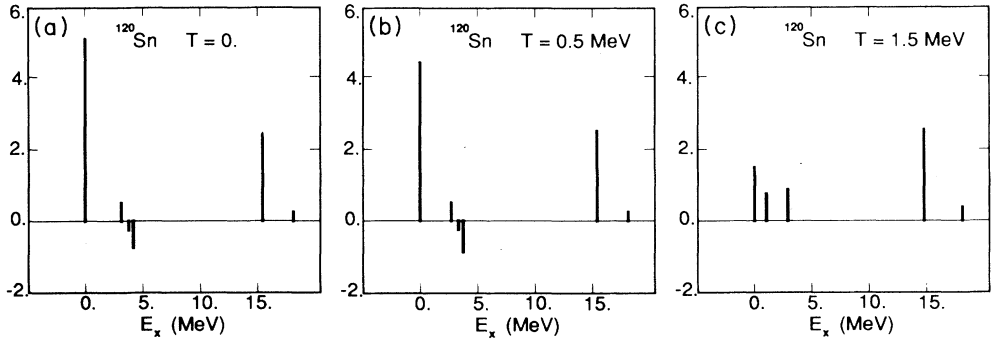

FIG. 7. Distribution of strength for stripping obtained from the solutions of the two quasiparticle RPA, at zero temperature [part (a)], for $T < T_c$ [part (b)], and for $T > T_c$ [part (c)].

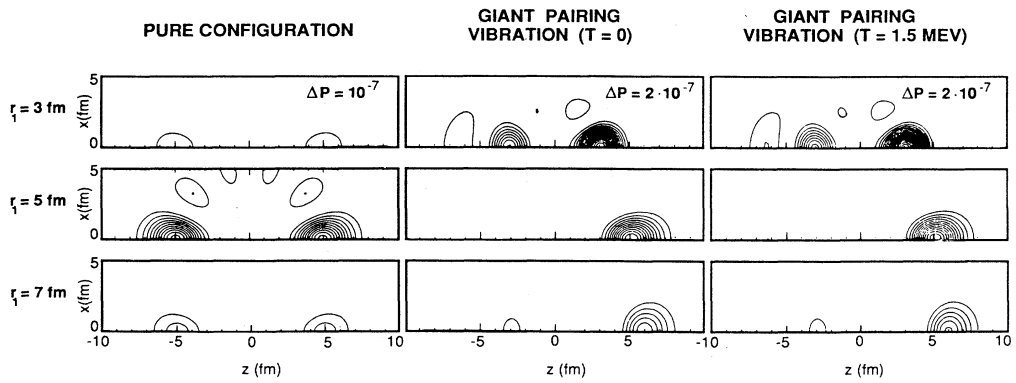

FIG. 8. Two-particle correlation plots associated with the giant pairing vibration in ^{120}Sn, for different values of the position of the first particle, at zero and finite temperatures (middle and right-hand side). The left-hand side refers to the case of uncorrelated particles, which in this case are expected to move in the $0h_{9/2}$ orbital.

This relation parallels the BCS prediction,[20] although it should be associated with a different Debye energy scale, being, in the case of a metallic superconductor, ω_D of the order of 0.02 eV.

The phase transition results in drastic changes in the spatial particle-particle correlation of the Cooper pairs. The two-particle probability distribution is obtained from Eq. (1) with

$$A_j^{(pv)}=\Omega_j^{1/2}u_j^{(A)}v_j^{(A+2)}(1-2f_j)\ , \tag{10}$$

when the temperature is below the critical value T_c, i.e., in the superfluid phase. For $T>T_c$, i.e., in the normal phase, the expression of the amplitudes $A_j^{(pv)}$'s is the same as in Eq. (3). The corresponding correlation plots are displayed in the middle and on the right-hand side of Fig. 6 for zero temperature and for a temperature just above the critical value. While in the superfluid phase there is a large increase of collectivity with respect to the pure configuration (the associated transition densities are expected to scale approximately by a factor of the order $\Delta/G\sim 10$), in the normal phase the results are practically the same as in the case of pure configuration. This is because in open-shell nuclei like ^{118}Sn, no single-particle gap in the nuclear spectrum exists, and thus the difference between particles and holes is blurred.

In Fig. 7 we display the distribution of strength for stripping processes obtained in the framework of finite temperature two-quasiparticle RPA for pairing modes[8,13]

$$A_j^{(pv)}=(u_j^{(A)2}X_j-v_j^{(A)2}Y_j)(1-2f_j)\ . \tag{11}$$

As apparent from the figure, collective states (giant pairing resonances) are present in the high part of the spectrum. The collectivity of these states is reflected in the associated correlation plots displayed in Fig. 8.

For $T>T_c$ the expression for the $A_j^{(pv)}$'s is the same as given in Eq. (3). For all values of T ($T\leq 3$ MeV), the collectivity of the giant pairing vibration, as expected, remains unchanged.

IV. CONCLUSIONS

The effects of temperature on the collectivity induced by pairing interaction are clearly seen in the changes displayed by the spatial distribution of the pair of nucleons forming the associated Cooper pairs. In both normal and superfluid nuclear systems low-lying pairing vibrations are strongly affected by temperatures of the order of 1–3 MeV. Giant pairing resonances, on the other hand, remain practically unchanged as temperature is increased.

[1]A. L. Goodman, in *Proceedings of Nuclear Summer Workshop, Santa Barbara, 1981,* edited by G. F. Bertsch (World Scientific, Singapore, 1982), and references therein.

[2]J. L. Egido, H. J. Mang, and P. Ring, Nucl. Phys. **A339**, 390 (1980); **A341**, 229 (1980); J. L. Egido and P. Ring, *ibid.* **A383**, 183 (1982); **A388**, 19 (1982); U. Mutz and P. Ring, J. Phys. G **10**, 139 (1984).

[3]R. S. Nikam, P. Ring, and L. F. Canto, Z. Phys. A **324**, 241 (1986); Phys. Lett. B **185**, 269 (1987); R. S. Nikam and P. Ring, Phys. Rev. Lett. **58**, 980 (1987).

[4]R. A. Broglia, in *Theory of Nuclear Structure and Reactions,* edited by M. Lozano and G. Madurga (World Scientific, Singapore, 1985), p. 133; R. A. Broglia, M. Diebel, S. Frauendorf, and M. Gallardo, Phys. Lett. **166B**, 252 (1986).

[5]R. A. Broglia, M. Diebel, S. Frauendorf, and F. Barranco, in *Proceedings of the XXIII Winter Meeting on Nuclear Physics, Bormio,* edited by I. Iori (Ricerca Scientifica ed Educazione Permanente, Milano, 1985), p. 1; E. Vigezzi, D. R. Bès, R. A. Broglia, and S. Frauendorf, Phys. Rev. C **38**, 1448 (1988).

[6]D. R. Bès and R. A. Broglia, Nucl. Phys. **80**, 289 (1966).

[7]F. Barranco, M. Gallardo, and R. A. Broglia, Phys. Lett. B **198**, 19 (1988); Y. R. Shimizu, E. Vigezzi, and R. A. Broglia, *ibid.* **198**, 33 (1987); Y. R. Shimizu, J. Garrett, R. A. Broglia, M. Gallardo, and E. Vigezzi, Rev. Mod. Phys. **61**, 131 (1989).

[8]O. Civitarese, G. G. Dussel, and R. P. J. Perazzo, Nucl. Phys. **A404**, 15 (1983); F. Alasia, O. Civitarese, and M. Reboiro, Phys. Rev. C **35**, 812 (1987).
[9]R. A. Broglia and D. R. Bès, Phys. Lett. **69B**, 129 (1977); M. W. Herzog, R. J. Liotta, and L. J. Sibanda, Phys. Rev. C **31**, 259 (1985); P. F. Bortignon, E. Maglione, A. Vitturi, F. Zardi, and R. A. Broglia, Phys. Scr. **34**, 678 (1986).
[10]G. F. Bertsch, R. A. Broglia, and C. Riedel, Nucl. Phys. **A91**, 123 (1967).
[11]F. Catara, A. Insolia, E. Maglione, and A. Vitturi, Phys. Rev. C **29**, 1091 (1984).
[12]L. Ferreira, R. J. Liotta, C. H. Dasso, R. A. Broglia, and A. Winther, Nucl. Phys. **A426**, 276 (1984).
[13]R. A. Broglia (unpublished).
[14]G. M. Crawley, W. Benenson, D. Weber, and B. Zwieglinski, Phys. Rev. Lett. **39**, 1451 (1977).
[15]M. W. Herzog, O. Civitarese, L. Ferreira, R. J. Liotta, T. Vertse, and L. J. Sibanda, Nucl. Phys. **A448**, 441 (1986); C. H. Dasso and R. J. Liotta, Phys. Rev. C **36**, 448 (1987).
[16]H. Sagawa and G. F. Bertsch, Phys. Lett. **146B**, 138 (1984); O. Civitarese, R. A. Broglia, and C. H. Dasso, Ann. Phys. (N.Y.) **156**, 142 (1984), and references therein.
[17]D. R. Bès, P. Lotti, E. Maglione, and A. Vitturi, Phys. Lett. **169B**, 5 (1986).
[18]M. D. Scadron, Ann. Phys. (N.Y.) **159**, 184 (1985).
[19]P. Decowski, W. Grochulski, A. Marcinkowski, K. Siwek, and Z. Wilhelmi, Nucl. Phys. **A110**, 129 (1968).
[20]J. Bardeen, L. Cooper, and J. Schrieffer, Phys. Rev. **106**, 162 (1957).